Armenian Journal of Physics, 2010, vol. 3, issue 1, pp. 45–60

SPIN EDGE STATES INDUCED BY THE SPIN-ORBIT INTERACTION AND ZEEMAN EFFECT IN RESTRICTED TWO-DIMENSIONAL ELECTRON SYSTEMS

V.L. Grigoryan

Yerevan State University, Yerevan, Armenia

(Received March 11, 2010)

Abstract - We study the spin edge states, induced by the combined effect of Bychkov-Rashba spin-orbit and Zeeman interactions or of Dresselhaus spin-orbit and Zeeman interactions in a two-dimensional electron system, exposed to a perpendicular quantizing magnetic field and restricted by a hard-wall confining potential. An exact analytical formula is derived for the dispersion relations of spin edge states and their energy spectrumis analyzed versus the momentum and the magnetic field. We calculate the average spincomponents and the average transverse position of electron. It is shown that by removing the spin degeneracy, spin-orbit interaction splits the spin edge states not only in the energy but also induces their spatial separation. Depending on the type of spin-orbit coupling and the major quantum number, the Zeeman termin the combination with spin-orbit interaction increases or decreases essentially the splitting of bulk Landau levels while it has a weak influence on the spin edge states.

Keywords:Two-dimensional electron system, spin edge state, spin-orbit interaction, confining potential, quantizing magnetic field, Zeeman effect

1. Introduction

The principal importance of spin-orbit interaction (SOI) is in its ability to link the electron charge and spin degrees of freedom, which is fertile for novel physical phenomena [1–3]. Unlike the charge, the electron spin is double-valued and identifies two system components, which can be separated as in the spin-Hall effect [4,5] and spin Hall drag effect [6] or mixed via the spin-Coulomb drag [7,8]. There are different mechanisms, realizing SOI[1], and the interplay between them produces another rich arena for study and potential applications in spintronics[9,10].

An effective way for realizing a control and manipulation of spin motion in spintronic device structures is based on the electrically tunable SOI when electron spins are affected by the electric field via the associated magnetic field in electron's rest frame. SOI plays a key role in spin relaxation, transport, and optical phenomena, which are currently actively studied for completely new applications in semiconductor spintronics [1-3].

Investigations of SOI induced effects in two-dimensional electron systems (2DES), exposed to a perpendicular magnetic field, have been initially related to the bulk Landau levels: the SOI renormalization of energy dispersions, the interplay between different SOI mechanisms, themagnetotransport and electron-electron interaction effects have attracted much attention [11-17]. In the quantum Hall effect geometry, however, the extended edge state plays an essential role in understanding of transport phenomena [18-21].

There are several theoretical papers which address the effect of SOI on the edge states along sample boundaries [22-25] or along magnetic interfaces [26, 27]. These papers find unlikely an

exact analytical solution of the edge state problem and adopt different numerical approaches [23-25, 27], use a parabolic confining potential [26], or give an analytical approximation in the limit of strong magnetic fields [22] where SOI is a priori weak.

In our recent paper we have studied the spin edge states, induced by the combined effect of spin-orbit interaction and hard-wall confining potential, in a 2DES exposed to a perpendicular quantizing magnetic field [28]. Using parabolic cylindrical functions,we have derived an exact analytical formula for the dispersion relations of spin edge states. This work, however, neglects the Zeeman interaction and considers only one type of SOI: Bychkov-Rashba spin-orbit coupling.

Here we present an analytical solution to the spin edge states, induced by the combined effect of Bychkov-Rashbaor DresselhausSOI, Zeeman effect, and hard-wall confining potential in a 2DES, exposed to a perpendicular quantizing magnetic field. We derive an exact formula for the electron energy dispersions and calculate the spectral and transport properties of spin edge states.We show that at sufficiently large effective spin-orbit coupling strengths or, what is the same, at sufficiently low magnetic fields, the Stark splitting of spin-resolved edge states gives rise to the anti-crossings of high energy bands. We find that SOI gives rise to interesting new effects. By removing the spin degeneracy, SOI creates not only the splitting of edge states in the energy but also induces spatial separation of the spin-resolved edge states. This effect is missed in the approximate approach adopted in [22]. It is shown that the influence of Zeeman effect on the energy spectrumof spin edge statesdiffers from its influence on the quasibulk Landau levels. The influence of Zeeman effect on the edge states is weak. Depending on the SOI coupling constant (BR or D) and on the major quantum number, the Zeeman effect increases or reduces the splitting of bulk Landau levels. The developed approach here is equally applicable to the magnetic edge states along magnetic interfaces created by inhomogeneous magnetic fields.

2. Theoretical concept

We assume that the 2DES resides in a quantum well, formed in the (001) plane of a zincblende semiconductor heterostructure, and is exposed to a perpendicular homogeneous magnetic field $\mathbf{B} = \mathrm{B}_0\mathbf{z}$. The motion of electrons in the 2DES is confined by an infinite potential $V(x) = \infty$ for $x < 0$. Such a system can be described by a two-dimensional model Hamiltonian of the form

$$H = H_0 + H_{SOI} + H_Z, \tag{1}$$

where the Hamiltonian of a free particle in a quantizing magnetic field is

$$H_0 = \frac{\boldsymbol{\pi}^2}{2m^*}\hat{\tau}, \tag{2}$$

the spin-orbit interaction Hamiltonian

$$H_{SOI} = \alpha_R \left(\pi_x \hat{\sigma}_y - \pi_y \hat{\sigma}_x \right) + \alpha_D \left(\pi_x \hat{\sigma}_x - \pi_y \hat{\sigma}_y \right), \tag{3}$$

and Zeeman effect Hamiltonian

$$H_Z = \frac{g\mu_B}{2} \boldsymbol{\sigma} \mathbf{B} . \tag{4}$$

Here m^* denotes the electron effective mass. The electron kinetic momentum operator $\boldsymbol{\pi} = \mathbf{P} - (e/c)\mathbf{A}$ where $\mathbf{P} = -i\hbar\nabla$ is the canonical momentum. α_R and α_D are the Bychkov-Rashba and Dresselhaus spin-orbit coupling constants, respectively, g is Landé factor of electron and $\mu_B = e\hbar/2m_0 c$ is the Bohr magneton where m_0 is the free electron mass. We choose the Landau gauge so that the components of the vector potential are $\mathbf{A}(x) = (0, xB_0, 0)$, $\hat{\tau}$ is the unity matrix and $\boldsymbol{\sigma} = \left(\hat{\sigma}_x, \hat{\sigma}_y, \hat{\sigma}_z \right)$ the Pauli spin matrices. We assume also that electrons are confined to the lowest energy subband in the z-direction.

In the expanded form the Hamiltonian (1) is given by

$$\begin{aligned} H = \frac{1}{2m^*} \left[P_x^2 + \left(P_y - \frac{e}{c} x B_0 \right)^2 \right] \hat{\tau} + \alpha_R \left[P_x \hat{\sigma}_y - \left(P_y - \frac{e}{c} x B_0 \right) \hat{\sigma}_x \right] + \\ + \alpha_D \left[P_x \hat{\sigma}_x - \left(P_y - \frac{e}{c} x B_0 \right) \hat{\sigma}_y \right] + \frac{g\mu_B}{2} \sigma_z B_0 . \end{aligned} \tag{5}$$

Using the ansatz

$$\Psi(x, y) = e^{ik_y y} \chi_{k_y}(x), \tag{6}$$

we can reduce the two-dimensional Schrödinger equation $H\Psi = E\Psi$ to the one-dimensional problem. Here E is the electron total energy and k_y is the electron momentum in the y – direction. From expression (5) we have

$$\begin{aligned} \frac{\hbar^2}{2m^*} \left\{ \left[-\frac{\partial^2}{\partial x^2} + \left(k_y - \frac{e}{c\hbar} x B_0 \right)^2 \right] \hat{\tau} + \frac{2m^* \alpha_R}{\hbar} \left[-i \frac{\partial}{\partial x} \hat{\sigma}_y - \left(k_y - \frac{e}{c\hbar} x B_0 \right) \hat{\sigma}_x \right] + \right. \\ \left. + \frac{2m^* \alpha_D}{\hbar} \left[-i \frac{\partial}{\partial x} \hat{\sigma}_x - \left(k_y - \frac{e}{c\hbar} x B_0 \right) \hat{\sigma}_y \right] + \frac{m^* g \mu_B}{\hbar^2} \hat{\sigma}_Z B_0 \right\} \chi_{k_y}(x) = \varepsilon \chi_{k_y}(x). \end{aligned} \tag{7}$$

Here we discuss in parallel two experimentally realizable situations in 2DES in the presence of the Bychkov-Rashba SOI + Zeeman interaction and in the presence of the Dresselhaus SOI +Zeeman interaction. In dimensionless units Eq. (7) has the form

$$\begin{aligned} \frac{1}{2} \left\{ \left[-l_B^{\,2} \frac{d^2}{dx^2} + \left(k_y l_B - \frac{x}{l_B} \right)^2 \right] \hat{\tau} + \frac{2m^* l_B \alpha_R}{\hbar} \left[-i l_B \frac{d}{dx} \hat{\sigma}_y - \left(k_y l_B - \frac{x}{l_B} \right) \hat{\sigma}_x \right] + \right. \\ \left. + \frac{2m^* l_B \alpha_D}{\hbar} \left[-i l_B \frac{d}{dx} \hat{\sigma}_x - \left(k_y l_B - \frac{x}{l_B} \right) \hat{\sigma}_y \right] + \frac{m^* g \mu_B c}{e\hbar} \hat{\sigma}_Z \right\} \chi_{k_y}(x) = \frac{\varepsilon}{\hbar\omega_B} \chi_{k_y}(x). \end{aligned} \tag{8}$$

Inthe case of BR SOI+Zthe electron wave function $\chi_{k_y}(x)$ in the *x*-direction should satisfy the equation:

$$\left\{\left[\frac{d^2}{dx^2}+\nu+\frac{1}{2}-\frac{\left(x-X\left(k_y\right)\right)^2}{4}\right]\hat{\tau}+\gamma_R\left[i\frac{d}{dx}\hat{\sigma}_y-\frac{\left(x-X\left(k_y\right)\right)}{2}\hat{\sigma}_x\right]-\gamma_Z\hat{\sigma}_Z\right\}\chi_{k_y}(x)=0, \tag{9}$$

while in the case of D SOI+Z $\chi_{k_y}(x)$ in the *x*-direction should satisfy the following equation:

$$\left\{\left[\frac{d^2}{dx^2}+\nu+\frac{1}{2}-\frac{\left(x-X\left(k_y\right)\right)^2}{4}\right]\hat{\tau}+\gamma_D\left[i\frac{d}{dx}\hat{\sigma}_x-\frac{\left(x-X\left(k_y\right)\right)}{2}\hat{\sigma}_y\right]-\gamma_Z\hat{\sigma}_Z\right\}\chi_{k_y}(x)=0, \tag{10}$$

where the effective potential $V_{eff}=\left[x-X\left(k_y\right)\right]^2/4$ in the *x*-direction depends additionally on the wave vector k_y along the $y-$direction. In Eqs.(9) and(10) we express the energy $E\to(\nu+1/2)\hbar\omega_B$ in units of the cyclotron energy, $\hbar\omega_B=\hbar eB_0/m^*c$, and the length $x\to xl_B/\sqrt{2}$ in the magnetic length, $l_B\equiv\sqrt{\hbar c/eB_0}$. We introduce also the dimensionless Rashba and Dresselhaus SOI coupling constants $\gamma_R=\sqrt{2}\alpha_R/v_B$ and $\gamma_D=\sqrt{2}\alpha_D/v_B$ with the cyclotron velocity $v_B=\hbar/m^*l_B$, the Zeeman interaction constant $\gamma_Z=gm^*\mu_Bc/e\hbar$, and the dimensionless coordinate of the center of orbital rotation $X\left(k_y\right)=\sqrt{2}k_yl_B$.

Now we take into account explicitly that the eigenstates of Eqs. (9) and (10) are spinors,

$$\chi_{k_y}(x)=\begin{pmatrix}\chi_{1k_y}\left(x-X\left(k_y\right)\right)\\ \chi_{2k_y}\left(x-X\left(k_y\right)\right)\end{pmatrix}, \tag{11}$$

for Rashba SOI and

$$\tilde{\chi}_{k_y}(x)=\begin{pmatrix}\tilde{\chi}_{1k_y}\left(x-X\left(k_y\right)\right)\\ \tilde{\chi}_{2k_y}\left(x-X\left(k_y\right)\right)\end{pmatrix}, \tag{12}$$

for Dresselhaus SOI, whose components can be classified by the spin projection on certain quantization axis. Then we can write the Schrödinger equation for Rashba SOI in the following compact matrix form:

$$\begin{pmatrix}h_{\nu-} & -\gamma_Rh+\\ -\gamma_Rh- & h_{\nu+}\end{pmatrix}\begin{pmatrix}\chi_{1k_y}(z)\\ \chi_{2k_y}(z)\end{pmatrix}=0 \tag{13}$$

and for Dresselhaus SOI:

$$\begin{pmatrix}h_{\nu-} & i\gamma_Dh-\\ -i\gamma_Dh+ & h_{\nu+}\end{pmatrix}\begin{pmatrix}\tilde{\chi}_{1k_y}(z)\\ \tilde{\chi}_{2k_y}(z)\end{pmatrix}=0, \tag{14}$$

where we have introduced the operators

$$h_{\nu\pm}=\left(\frac{d^2}{dz^2}+\nu+\frac{1}{2}-\frac{z^2}{4}\pm\gamma_Z\right), \tag{15}$$

$$h_{\pm}=\left[\frac{z}{2}\mp\frac{d}{dz}\right]. \tag{16}$$

The systems of equations in (13) and (14) have to be solved under the boundary conditions $\chi_{k_y}(x)\to 0$ and $\tilde{\chi}_{k_y}(x)\to 0$ when $x\to 0$ and $x\to+\infty$. In the absence of SOI, $h_{\pm}=0$, the solution is given in terms of the parabolic cylindrical functions, $D_{\nu}(x)$. In the presence of SOI we search the bulk solution of matrix equations (13) and (14) as

$$\chi_{1k_y}(z)=aD_{\mu}(z), \tag{17}$$

$$\chi_{2k_y}(z)=bD_{\mu-1}(z), \tag{18}$$

$$\tilde{\chi}_{1k_y}(z)=\tilde{a}D_{\tilde{\mu}-1}(z), \tag{19}$$

$$\tilde{\chi}_{2k_y}(z)=\tilde{b}D_{\tilde{\mu}}(z). \tag{20}$$

Here a, b and $\tilde{a}, \tilde{b}$ are the spinor coefficients and do not depend on *x*. In general μ and $\tilde{\mu}$ are arbitrary indices, different from ν. Making use the following recurrent properties of the parabolic cylindrical functions:

$$h_{\nu\pm}D_{\mu}(z)=(\nu-\mu\pm\gamma_Z)D_{\mu}(z), \tag{21}$$

$$h_{\pm}D_{\mu}(z)=\begin{cases}D_{\mu+1}(z)\\ \mu D_{\mu-1}(z)\end{cases}, \tag{22}$$

for Rashba SOI we obtain from Eq. (13) the system of equations

$$\begin{cases}\left[a(\nu-\mu-\gamma_Z)-b\gamma_R\right]D_{\mu}(z)=0,\\ \left[b(\nu+1-\mu+\gamma_Z)-a\gamma_R\mu\right]D_{\mu-1}(z)=0\end{cases} \tag{23}$$

and for Dresselhaus SOI from Eq. (14) we obtain the following system of equations:

$$\begin{cases}\left[\tilde{a}(\nu-\tilde{\mu}+1-\gamma_Z)+i\tilde{b}\tilde{\mu}\gamma_D\right]D_{\tilde{\mu}-1}(z)=0,\\ \left[\tilde{b}(\nu-\tilde{\mu}+\gamma_Z)-i\tilde{a}\gamma_D\right]D_{\tilde{\mu}}(z)=0.\end{cases} \tag{24}$$

The solutions of the above systems give

$$\mu_{\pm}(\nu,\gamma_R,\gamma_Z)=\nu+\frac{1}{2}+\frac{\gamma_R^2}{2}\pm\sqrt{\nu\gamma_R^2+\frac{1}{4}\left(1+\gamma_R^2\right)^2+\gamma_Z(\gamma_Z+1)}, \tag{25}$$

$$c_{\pm}(\nu,\gamma_R,\gamma_Z)=-\frac{1}{\gamma_R}\left(\frac{1}{2}+\frac{\gamma_R^2}{2}+\gamma_Z\pm\sqrt{\nu\gamma_R^2+\frac{1}{4}\left(1+\gamma_R^2\right)^2+\gamma_Z(\gamma_Z+1)}\right) \tag{26}$$

for Rashba SOI and

$$\tilde{\mu}_{\pm}(\nu,\gamma_R,\gamma_Z)=\nu+\frac{1}{2}+\frac{\gamma_D^2}{2}\pm\sqrt{\nu\gamma_D^2+\frac{1}{4}\left(1+\gamma_D^2\right)^2+\gamma_Z\left(\gamma_Z-1\right)}, \tag{27}$$

$$\tilde{c}_{\pm}^{1}(\nu,\gamma_R,\gamma_Z)=i\frac{1}{\gamma_R}\left(\frac{1}{2}+\frac{\gamma_D^2}{2}-\gamma_Z\pm\sqrt{\nu\gamma_D^2+\frac{1}{4}\left(1+\gamma_D^2\right)^2+\gamma_Z\left(\gamma_Z-1\right)}\right)\equiv i\tilde{c}_{\pm} \tag{28}$$

for Dresselhaus SOI where $c_{\pm}=b_{\pm}/a_{\pm}$ and $\tilde{c}^{1}{}_{\pm}=\tilde{a}_{\pm}/\tilde{b}_{\pm}$. Thus, the two independent bulk solutions of Eq. (13) are given by the spinor wave functions

$$\chi_{k_y}^{\pm}(z)=a_{\pm}\begin{vmatrix} D_{\mu\pm(\nu,\gamma_R,\gamma_Z)}(z) \\ c_{\pm}D_{\mu\pm(\nu,\gamma_R,\gamma_Z)-1}(z)\end{vmatrix}, \tag{29}$$

and solutions of Eq. (14) by the spinor wave functions

$$\tilde{\chi}_{k_y}^{\pm}(z)=\tilde{b}_{\pm}\begin{vmatrix} i\tilde{c}_{\pm}D_{\tilde{\mu}\pm(\nu,\gamma_R,\gamma_Z)-1}(z) \\ D_{\tilde{\mu}\pm(\nu,\gamma_R,\gamma_Z)}(z)\end{vmatrix}. \tag{30}$$

The normalization of the wave functions for Rashba SOI

$$\int dz\chi_{k_y}^{*}(z)\chi_{k_y}(z)=1 \tag{31}$$

and for Dresselhaus SOI

$$\int dz\tilde{\chi}_{k_y}^{*}(z)\tilde{\chi}_{k_y}(z)=1 \tag{32}$$

gives the amplitudes of eigenstates for Rashba SOI andfor Dresselhaus SOI.

$$a_{\pm}=\left[\int dz\left(\left|D_{\mu\pm}(z)\right|^2+\left|c_{\pm}\right|^2\left|D_{\mu\pm-1}{}^2\right|\right)\right]^{-1/2}, \tag{33}$$

$$\tilde{b}_{\pm}=\left[\int dz\left(\left|D_{\tilde{\mu}\pm}(z)\right|^2+\left|\tilde{c}_{\pm}\right|^2\left|D_{\tilde{\mu}\pm-1}{}^2\right|\right)\right]^{-1/2}. \tag{34}$$

One can see that in the limit of vanishing SOI, $\gamma_R(\gamma_D)\to 0$, we have $a_{+}(\tilde{a}_{+})\to 0$ and $b_{-}(\tilde{b}_{-})\to 0$ and recover the usual magnetic edge states, which are doubly degenerated with respect to spin,

$$\chi_{k_y}^{+}(x)\sim D_{\nu}(x)\begin{pmatrix}1\\0\end{pmatrix}, \tag{35}$$

$$\chi_{k_y}^{-}(x)\sim D_{\nu}(x)\begin{pmatrix}0\\1\end{pmatrix}. \tag{36}$$

On the other hand, solution (29) for sufficiently large values of $X(k_y)$ describes quasibulk Landau states so that the index $\mu_{\pm}(\nu,\gamma_R)$ differs only exponentially from Landau index $l=0,1,2,...$ and the parabolic cylindric functions are given by their asymptotics Hermitepolynomials $D_l(\xi)=2^{-l/2}\exp\left(-\xi^2/4\right)H_l\left(\sqrt{\xi}/2\right)$. In the limit of $X(k_y)\to\infty$, taking $\mu_{\pm}(\nu,\gamma_R)=l$ in Eqs. (25) and

(26), one can exactly reproduce the spectrum and the wave functions of the bulk dispersionless Landau levels, renormalized by the SOI and Zeeman effect for $l = 1,2,...$:

$$E_l^{\pm}(\gamma) = l \pm \sqrt{\frac{1}{4} + \gamma^2 l + \gamma_z(\gamma_z + 1)}, \tag{37}$$

$$c_{\pm}(\nu,\gamma) = -\frac{1}{2\gamma}\left(1 + 2\gamma_z \mp 2\sqrt{\frac{1}{4} + \gamma^2 l + \gamma_z(\gamma_z + 1)}\right). \tag{38}$$

As usual the $l = 0$ Landau level remains not perturbed by the spin-orbit coupling.

In order to obtain the single particle spectrum of the spin edge states, we have to require vanishing of the electron wave functions (29) and (30) at $x = 0$. Since the time-dependent spinor wave functions are the solutions of the time-dependent Schrödinger equation, the energy E, obtained from the vanishing condition of both spinor components, should be the same. As seen, however, from Eqs. (29) and (30), the different spinor components of the bulk solution are given by the parabolic cylindrical functions with different indices. This makes impossible vanishing of the spinor components of functions (29) and (30) simultaneously. In order to satisfy the boundary conditions at $x = 0$ and to obtain the energy spectrum of spin edge states, we construct a linear combination of the two independent bulk solutions as

$$\Psi_{k_y}(z) = \alpha\chi^{+}_{k_y}(z) + \beta\chi^{-}_{k_y}(z) \tag{39}$$

and

$$\tilde{\Psi}_{k_y}(z) = \tilde{\alpha}\tilde{\chi}^{+}_{k_y}(z) + \tilde{\beta}\tilde{\chi}^{-}_{k_y}(z) \tag{40}$$

for Rashba and Dresselhaus SOI, respectively, and choose the coefficients α,β and $\tilde{\alpha},\tilde{\beta}$ so that the new spinor wave functions $\Psi_{k_y}(z)$ and $\tilde{\Psi}_{k_y}(z)$ vanish at $x = 0$. The eigenvalue problem for α,β or $\tilde{\alpha},\tilde{\beta}$ has a solution if the corresponding determinant vanishes at $x = 0$. This leads to the following exact dispersion equations for the spin edge states for Rashba SOI:

$$c_{-}D_{\mu_{+}}\left(-X(k_y)\right)D_{\mu_{-}-1}\left(-X(k_y)\right) = c_{+}D_{\mu_{-}}\left(-X(k_y)\right)D_{\mu_{+}-1}\left(-X(k_y)\right) \tag{41}$$

and

$$\tilde{c}^{1}_{-}D_{\tilde{\mu}_{+}}\left(-X(k_y)\right)D_{\tilde{\mu}_{-}-1}\left(-X(k_y)\right) = \tilde{c}^{1}_{+}D_{\tilde{\mu}_{-}}\left(-X(k_y)\right)D_{\tilde{\mu}_{+}-1}\left(-X(k_y)\right) \tag{42}$$

for Dresselhaus SOI. Recall that the dependence on the energy $E \to (\nu + 1/2)\hbar\omega_B$ manifests itself via the functions $\mu_{\pm}(\nu,\gamma)$ and $c_{\pm}(\nu,\gamma)$ for Rashba SOI and $\tilde{\mu}_{\pm}(\nu,\gamma)$ and $\tilde{c}^{1}_{\pm}(\nu,\gamma) = i\tilde{c}_{\pm}(\nu,\gamma)$ for Dresselhaus SOI given by Eqs. (25), (26) and Eqs. (27), (28), respectively. The dispersion relations (41) and (42) are quadratic with respect to the parabolic cylindrical functions, therefore for a given band index n it has two solutions, $E_{sn}(k_y)$, corresponding to the magnetic edge states with the

$s = \uparrow$ and $\downarrow$ spins. In weak magnetic fields the Zeeman effect is small. If we do not consider it, taking $\gamma_Z = 0$, then formulas (25) and (26) will have the following forms: for Rashba SOI

$$\mu_{\pm}\left(\nu,\gamma_R,\gamma_Z\right) = \nu + \frac{1}{2} + \frac{\gamma_R^2}{2} \pm \sqrt{\nu\gamma_R^2 + \frac{1}{4}\left(1+\gamma_R^2\right)^2}, \tag{43}$$

$$c_{\pm}\left(\nu,\gamma_R,\gamma_Z\right) = -\frac{1}{\gamma_R}\left(\frac{1}{2} + \frac{\gamma_R^2}{2} \pm \sqrt{\nu\gamma_R^2 + \frac{1}{4}\left(1+\gamma_R^2\right)^2}\right) \tag{44}$$

and for Dresselhaus SOI

$$\tilde{\mu}_{\pm}\left(\nu,\gamma_D,\gamma_Z\right) = \nu + \frac{1}{2} + \frac{\gamma_D^2}{2} \pm \sqrt{\nu\gamma_D^2 + \frac{1}{4}\left(1+\gamma_D^2\right)^2}, \tag{45}$$

$$\tilde{c}_{\pm}^{1}\left(\nu,\gamma_D,\gamma_Z\right) = i\frac{1}{\gamma_D}\left(\frac{1}{2} + \frac{\gamma_D^2}{2} \pm \sqrt{\nu\gamma_D^2 + \frac{1}{4}\left(1+\gamma_D^2\right)^2}\right) = i\tilde{c}_{\pm}. \tag{46}$$

We construct the wave functions of the spin edge states for the Rashba SOI as

$$\Psi_{k_y}\left(z\right) = a\begin{pmatrix}\Psi_{\uparrow k_y}\left(z\right)\\ \Psi_{\downarrow k_y}\left(z\right)\end{pmatrix}, \tag{47}$$

with the spinor components

$$\begin{aligned}\Psi_{\uparrow k_y}\left(z\right) &= D_{\mu_+}\left(z\right) - rD_{\mu_-}\left(z\right),\\ \Psi_{\downarrow k_y}\left(z\right) &= c_+ D_{\mu_+ -1}\left(z\right) - rc_- D_{\mu_- -1}\left(z\right)\end{aligned} \tag{48}$$

and for the Dresselhaus SOI as

$$\tilde{\Psi}_{k_y}\left(z\right) = \tilde{b}\begin{pmatrix}i\tilde{\Psi}_{\uparrow k_y}\left(z\right)\\ \tilde{\Psi}_{\downarrow k_y}\left(z\right)\end{pmatrix}, \tag{49}$$

with the spinor components

$$\begin{aligned}\Psi_{\uparrow k_y}\left(z\right) &= \tilde{c}_+^1 D_{\tilde{\mu}_+ -1}\left(z\right) - \tilde{r}\tilde{c}_-^1 D_{\tilde{\mu}_- -1}\left(z\right),\\ \tilde{\Psi}_{\downarrow k_y}\left(z\right) &= D_{\tilde{\mu}_+}\left(z\right) - \tilde{r}D_{\tilde{\mu}_-}\left(z\right),\end{aligned} \tag{50}$$

where $r = D_{\mu_+}\left(-X\left(k_y\right)\right)\Big/D_{\mu_-}\left(-X\left(k_y\right)\right)$ and $\tilde{r} = D_{\tilde{\mu}_+}\left(-X\left(k_y\right)\right)\Big/D_{\tilde{\mu}_-}\left(-X\left(k_y\right)\right)$. In Eqs. (47) and (48) $\mu_{\pm}\left(\nu,\gamma\right), c_{\pm}\left(\nu,\gamma\right)$ and $\mu_{\pm}\left(\nu,\gamma\right), \tilde{c}_{\pm}^{1}\left(\nu,\gamma\right) = i\tilde{c}_{\pm}\left(\nu,\gamma\right)$ have the form expressed in Eqs. (25), (26) and (27), (28), respectively, in the presence of Zeeman effect and in Eqs. (43), (44) and (45), (46) in the absence of Zeeman effect. Having the wave functions, we calculate the average spin components along the x, y, z-directions:

$$S_{sn}^{x,y,z}\left(k_y\right) = \frac{\hbar}{2}\int_0^{\infty} dx\Psi_{k_y}^{\dagger}\left(z\right)\sigma_{x,y,z}\Psi_{k_y}\left(z\right)\Big|_{E=E_{sn}\left(k_y\right)} \tag{51}$$

Since the transverse wave functions for the Rashba SOI are real, then $\Psi_{k_y}^{\dagger}(z)=\Psi_{k_y}^{T}(z)$ where $\Psi_{k_y}^{T}(z)$ is the transpose of wave function spinor, and the average spin component in the x-direction has the form

$$\begin{aligned} S_{sn}^{x}(k_y)&=\frac{\hbar}{2}\int_0^{\infty}dx\Psi_{k_y}^{*}(z)\sigma_x\Psi_{k_y}(z)\Big|_{E=E_{sn}(k_y)} \\ &=\frac{\hbar}{2}\int_0^{\infty}dx\Big[\Psi_{\uparrow k_y}(z)\Psi_{\downarrow k_y}(z)+\Psi_{\downarrow k_y}(z)\Psi_{\uparrow k_y}(z)\Big]\Big|_{E=E_{sn}(k_y)}= \\ &=\hbar\int_0^{\infty}dx\Big[\Psi_{\uparrow k_y}(z)\Psi_{\downarrow k_y}(z)\Big]\Big|_{E=E_{sn}(k_y)}, \end{aligned} \tag{52}$$

in the y-direction

$$\begin{aligned} S_{sn}^{y}(k_y)&=\frac{\hbar}{2}\int_0^{\infty}dx\Psi_{k_y}^{\dagger}(z)\sigma_y\Psi_{k_y}(z)\Big|_{E=E_{sn}(k_y)} \\ &=\frac{\hbar}{2}\int_0^{\infty}dx\Big[-i\Psi_{\uparrow k_y}(z)\Psi_{\downarrow k_y}(z)+i\Psi_{\downarrow k_y}(z)\Psi_{\uparrow k_y}(z)\Big]\Big|_{E=E_{sn}(k_y)}=0, \end{aligned} \tag{53}$$

and in the z-direction

$$S_{sn}^{z}(k_y)=\frac{\hbar}{2}\int_0^{\infty}dx\Psi_{k_y}^{\dagger}(z)\sigma_z\Psi_{k_y}(z)\Big|_{E=E_{sn}(k_y)}=\frac{\hbar}{2}\int_0^{\infty}dx\Big[\Psi_{\uparrow k_y}^{2}(z)-\Psi_{\downarrow k_y}^{2}(z)\Big]\Big|_{E=E_{sn}(k_y)}. \tag{54}$$

For the Dresselhaus SOI the transverse wave functions are imaginary, so $\Psi_{k_y}^{\dagger}(z)=\Psi_{k_y}^{*T}(z)$ where $\Psi_{k_y}^{*}(z)$ is the complex conjugate of wave functions and the average spin component in the x-direction has the form:

$$\begin{aligned} \tilde{S}_{sn}^{x}(k_y)&=\frac{\hbar}{2}\int_0^{\infty}dx\tilde{\Psi}_{k_y}^{\dagger}(z)\sigma_x\tilde{\Psi}_{k_y}(z)\Big|_{E=E_{sn}(k_y)} \\ &=\frac{\hbar}{2}\int_0^{\infty}dx\Big[-i\tilde{\Psi}_{\uparrow k_y}(z)\tilde{\Psi}_{\downarrow k_y}(z)+i\tilde{\Psi}_{\downarrow k_y}(z)\tilde{\Psi}_{\uparrow k_y}(z)\Big]\Big|_{E=E_{sn}(k_y)}=0, \end{aligned} \tag{55}$$

in the y-direction

$$\begin{aligned} \tilde{S}_{sn}^{y}(k_y)&=\frac{\hbar}{2}\int_0^{\infty}dx\tilde{\Psi}_{k_y}^{\dagger}(z)\sigma_y\Psi_{k_y}(z)\Big|_{E=E_{sn}(k_y)} \\ &=\frac{\hbar}{2}\int_0^{\infty}dx\Big[-\tilde{\Psi}_{\downarrow k_y}(z)\tilde{\Psi}_{\uparrow k_y}(z)-\tilde{\Psi}_{\uparrow k_y}(z)\tilde{\Psi}_{\downarrow k_y}(z)\Big]\Big|_{E=E_{sn}(k_y)}= \\ &=-\hbar\int_0^{\infty}dx\Big[\tilde{\Psi}_{\uparrow k_y}(z)\tilde{\Psi}_{\downarrow k_y}(z)\Big]\Big|_{E=E_{sn}(k_y)}, \end{aligned} \tag{56}$$

and in the z-direction

$$\tilde{S}_{sn}^{z}(k_y)=\frac{\hbar}{2}\int_0^{\infty}dx\tilde{\Psi}_{k_y}^{*}(z)\sigma_z\tilde{\Psi}_{k_y}(z)\Big|_{E=E_{sn}(k_y)}=\frac{\hbar}{2}\int_0^{\infty}dx\Big[\tilde{\Psi}_{\uparrow k_y}^{2}(z)-\tilde{\Psi}_{\downarrow k_y}^{2}(z)\Big]\Big|_{E=E_{sn}(k_y)}. \tag{57}$$

2. Spectrum of spin edge states

In this section we carry out the actual calculations of the spectrum of spin edge states. We also calculate the average spincomponents and the average transverse position of electron. The spin-orbit coupling for electrons in the conduction band of semiconductors is renormalized due to mixing of the valence bands into the dynamics of the conduction band. Despite the strong, by some six orders of magnitude, enhancement of the effective spin-orbit coupling, the spin-orbit effects remain as a weak perturbation in manysemiconductors. In the presence of a perpendicular magnetic field, the efficiency of SOI isdetermined by the dimensionless coupling constants γ_R, γ_D which are inversely proportional to the square root of the magnetic field strength, B_0. Here we carry the actual calculations for magnetic fields corresponding to the cyclotron splitting of about 5K. In InAswith the electron effective mass $m^* = 0.026m_0$ such a cyclotron splitting is achieved for B_0=0.1T and taking the Rashba constant $\alpha_R \approx 112.49$ meVÅ [1] we have for the Rashba coupling constant $\gamma_R = 0.45$. Taking $\alpha_D \approx 33.33$ meVÅ [1] we also calculate the Dresselhaus SOI constant $\gamma_D = 0.133$. Using the value of Lande factor $g = -15$ [29] for bulk InAswe calculate the Zeeman effect constant $\gamma_Z = -0.1$. As we will see below, such a strong relative coupling results in essential modifications of the spin edge state spectrum, which are measurable in experiment. The Bychkov-Rashba coupling constant can be changed by varying external electric field while the Dresselhaus coupling constant by varying the structural parameters. in order to be able to compare effectively the situations BR+Z and D+Z and to provide a clear understanding of the Zeeman effect on BR or D SOI separately, we carry out our calculations for the equal BR and D SOI strength, $\gamma_R = \gamma_D = 0.3$, and Zeeman coupling $\gamma_Z = 0.1$.

In Fig. 1 we plot the energy spectrum of spin edge states, $E_{sn}(k_y)$, as a function of momentum k_y, which we obtain by solving the dispersion equations (41) and (42) in the presence of Dresselhaus SOI and Zeeman effect (Fig. 1a) and Rashba SOI and Zeeman effect (Fig. 1b) for $\gamma_R = \gamma_D = 0.3$ and $\gamma_Z = 01$. It is seen that for a given quantum number n there are two spin resolved magnetic edge states, $E_{\downarrow n}(k_y)$ and $E_{\uparrow n}(k_y)$[28]. In the absence of Zeeman effectspecta of Rashba and Dresselhaus SOI are the same (black lines in Figs. 1a and 1b). The spin splitting of edge states increases with the main quantum number, n. Both branches show monotonic behavior in the whole range of k_y variation. For negative values of k_y, the spectrum describes the spin current-carrying skipping orbits. The influence of Zeeman effecton BR and D SOI for those values of k_y is weak. For large positive values of k_y, the energy of spin edge states is given by the spin-split quasibulk Landau levels. In this range of momentum k_y the influence of Zeeman effect for Rashba SOI

differs from that forDresselhaus SOI. It is seen that the splitting of energy levels for Dresselhaus SOI increases for all quantum numbers n, because of Zeeman effect (Fig. 1a). The situation is different in the case of Rashba SOI. For large positive values of k_y Zeeman effect reduces the splitting of energy for $n>1$ quantum numbers.

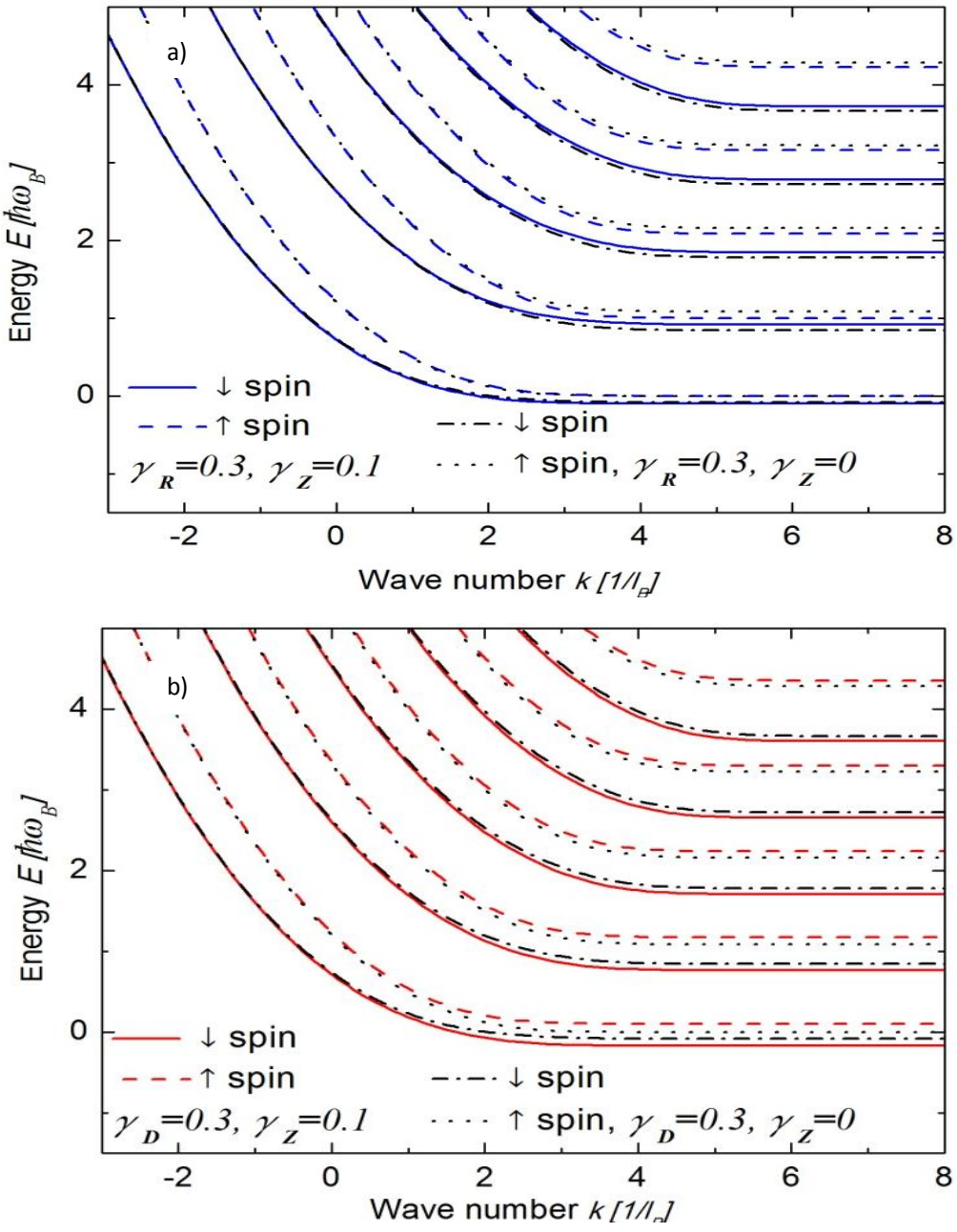

Fig. 1. (Color online) (a)The energy spectrum for Rashba SOI and Zeeman effect. Solid and dashed curves correspond to the down and up spins when $\gamma_R = 0.3$, $\gamma_Z = 0.1$, dash-dotted and dotted curves correspond to the down and up spins when $\gamma_R = 0.3$, $\gamma_Z = 0$ [28], (b)for Dresselhaus SOI and Zeeman effect. Solid and dashed curves correspond to the down and up spins when $\gamma_D = 0.3$, $\gamma_Z = 0.1$, dash-dotted and dotted curves correspond to the down and up spins when $\gamma_D = 0.3$, $\gamma_Z = 0$. The n = 5 lowest bands are shown.

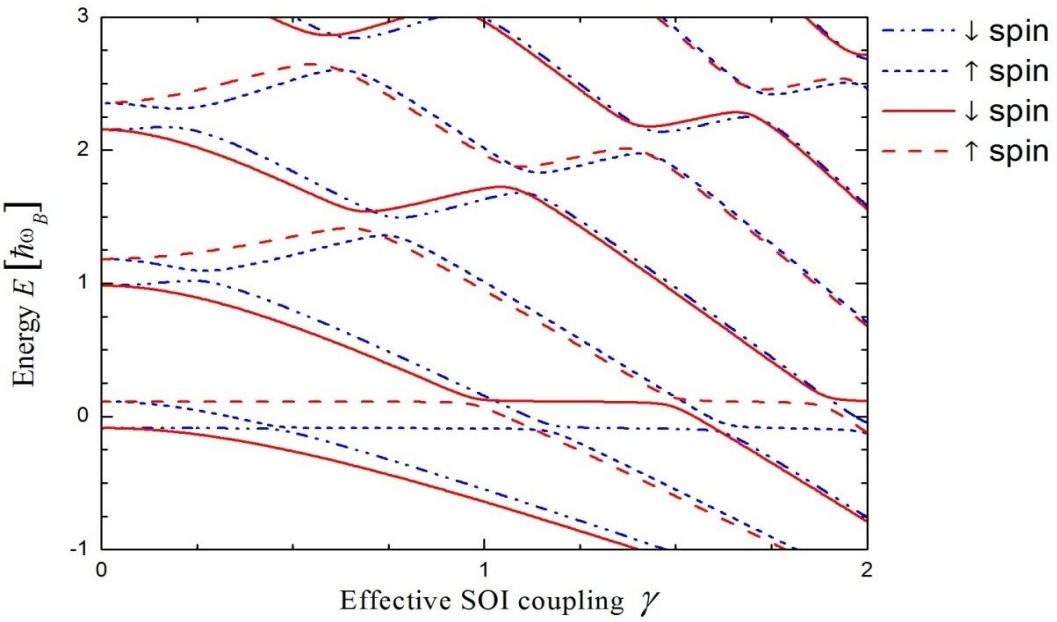

Fig. 2. (Color online)The energy spectrum of spin edge states as a function of the effective SOI coupling $\gamma_{R,D}$ (or what is the same, as a function of $B^{-1/2}$) for $X(k_y)=3$. The solid and dashed curves correspond to the down and up spin stateswhen $\gamma_D=0.3,\gamma_Z=0.1$, dash-dot-dot and short dashed curves correspond to the down and up spins when $\gamma_R=0.3,\gamma_Z=0.1$.

As it is shown in Ref. [28], for the stronger effective SOI coupling the energy spectrum shows well-pronounced anti-crossings. This phenomenon is observed also in the presence of Zeeman effect. The development of the anti-crossings can be traced clearly in Fig. 2 where we calculate the energy of spin edge states versus $\gamma_{R,D}$ or, what is the same, versus $1/\sqrt{B_0}$ for $\gamma_z=0.1$ and the fixed values of the guiding center coordinate, $X(k_y)=3$. The solid and dashed curves correspond to the down and up spin states for the case D+Z, dash-dot-dotted and short-dashed curves correspond to the down and up spins for BR+Z.One can see in Fig. 2 that depending on value of SOI coupling constant or magnetic field, the Zeeman effect can increase or decrease the splitting of energy levels. It is seen that at low values of SOI coupling the splitting of energy levels of the BR SOI and Zeeman interaction spin edge states decrease and show anticrossings, while the splitting of energy levels of D SOI and Zeeman interaction spin edge states increase. In Fig. 3 we plot the average transverse positions of the spin edge states from the boundary of 2DES in cases when $\gamma_D=0.3,\gamma_Z=0.1$ (Fig. 3a), $\gamma_R=0.3,\gamma_Z=0.1$ (Fig. 3b) and $\gamma_{D,R}=0.3,\gamma_Z=0$ (Fig. 3c) [28] as a function of their center of orbital motion, defined as

$$\Delta x_{sn}(k_y)=\int_0^\infty dx x\left|\Psi_{k_y}\left[x-X(k_y)\right]\right|^2_{E=E_{sn}(k_y)} \qquad (58)$$

It is seen from the figure that except for large positive values of k_y, the position of skipping

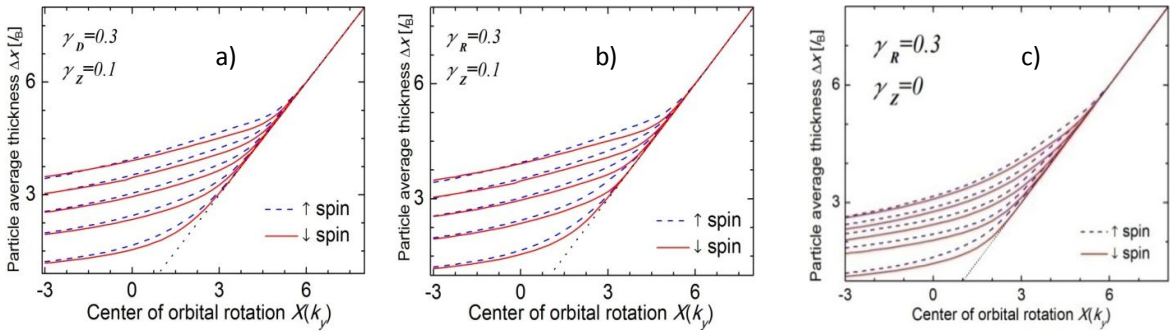

Fig. 3. The particle average position as a function of k_y for (a) $\gamma_D = 0.3, \gamma_Z = 0.1$ (b) $\gamma_R = 0.3, \gamma_Z = 0.1$, (c) $\gamma_{D,R} = 0.3, \gamma_Z = 0$ [28]. Solid and dashed curves correspond to the down and up spins.

orbits takes spin-resolved values in the absence of the Zeeman effect as well as in the presence of it, so that the up- and down-spin-edge states are separated in space.The differences in the probability density for different spins and wave vectors of the first two bands are clearly shown in Fig. 4. This effect appears also in the presence of Zeeman effect. As seen from Fig. 4b, the probability density for different bands and spins differs even at large positive values of k_y. In this limit, however, irrespective the quantum number *n* and the spin orientation, the particle average thickness is the same and varies linearly with its center of orbital motion. This is because in the quasibulk Landau states far from the interface, electrons oscillate symmetrically with respect to the guiding center, $X(k_y)$, independent of the spin and band index.

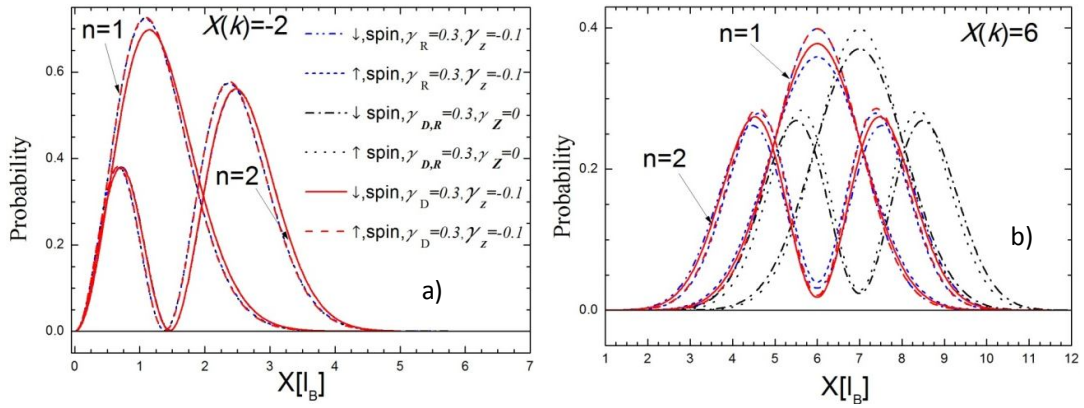

Fig. 4. (Color online) The particle probability density in the respective guiding orbit positions, a) $X(k) = -2$, b) $X(k) = 6$, as a function of *x*. The solid and dashed curves correspond to the down and up spin states when $\gamma_D = 0.3, \gamma_Z = 0.1$, dash-dotted and dotted curves correspond to the down and up spins when $\gamma_{D,R} = 0.3, \gamma_Z = 0$ [28], dash-dot-dot and short dashed curves correspond to the down and up spins when $\gamma_R = 0.3, \gamma_Z = 0.1$.

Notice the average transverse position of the spin edge states also takes spin-resolved values so that the up and down spin edge states are separated in space. From the obtained spectrum wecalculate average spin components along x, y, z -directions defined in (52)-(57). In Fig. 5 we plot $S_{sn}^{x,z}(k_y)$ for the case R+Z and $S_{sn}^{y,z}(k_y)$ for the case D+Z as a function of $X(k_y)$ when

$\gamma_D = 0.3, \gamma_Z = -0.1$, (a) $n = 1$, (b) $n = 2$, $\gamma_R = 0.3, \gamma_Z = -0.1$, and $\gamma_{D,R} = 0.3, \gamma_Z = 0$ for (c) $n = 1$ and (d) $n = 2$. As it is shown in Ref. [28], in the absence of Zeeman effect at large positive values of k_y when electrons are far from the hard wall, the spins are mainly aligned along *z*-axis. This is because in the quasibulk Landau states electrons have no preferential direction in the x, y plane of their cyclotron rotation. In the opposite limit of negative k_y, the edge channels are formed and the spins are mainly aligned in the x-direction, perpendicular to the y-direction of electron propagation. The situation is the same for Rashba SOI in the presence of Zeeman effect, because $S_{sn}^{y}(k_y) = 0$ (53). For Dresselhaus SOI and Zeeman effect $S_{sn}^{x}(k_y) = 0$ (55) and in the limit of negative k_y, spins are mainly aligned in the y-direction parallel to the direction of electron propagation. Notice that due to the spin splitting the absolute values of the average spin components do not equal in the up and down states and this asymmetry becomes stronger with the band index n.

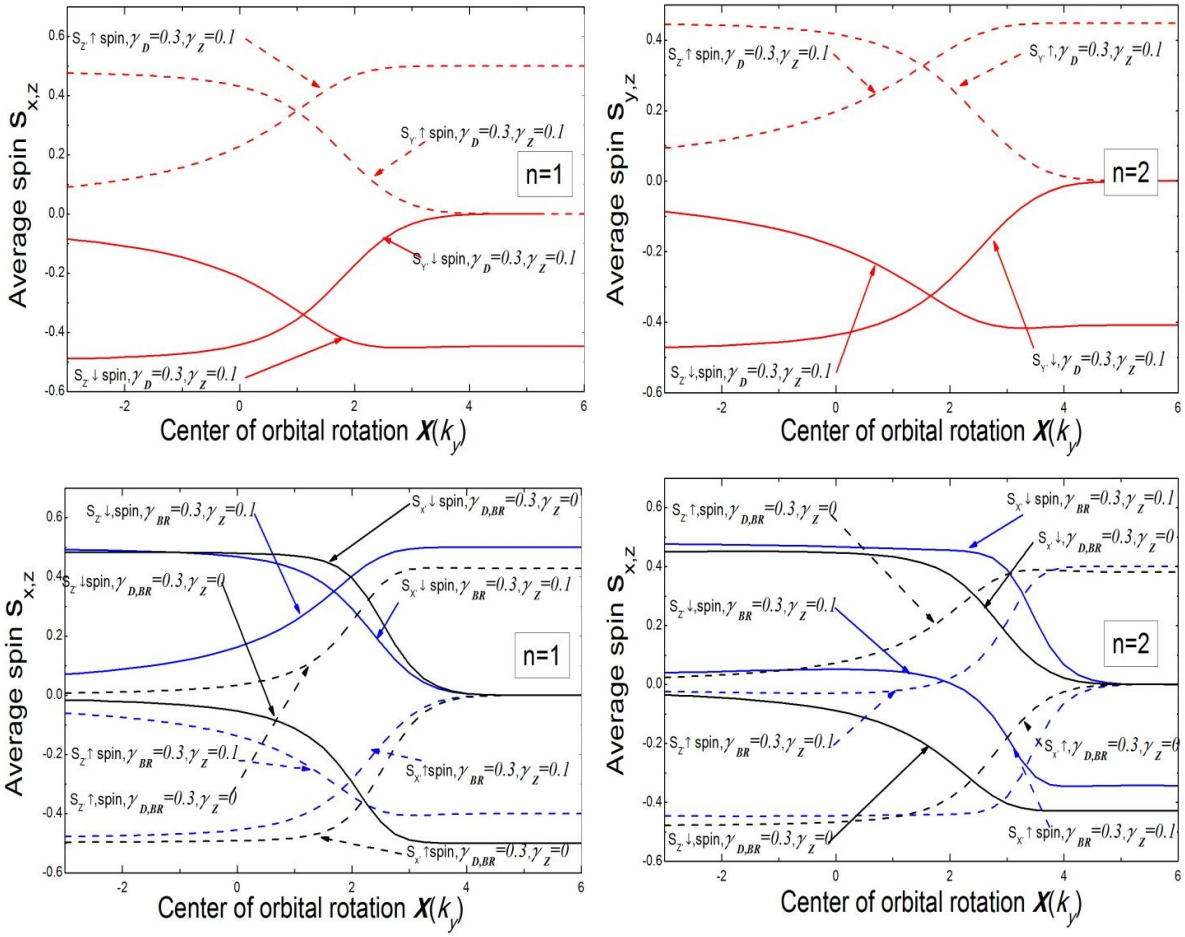

Fig. 5. The *x,y* and *y,z* components of average spins in units of ħ as a function of $X(k_y)$ for the first two bands (a) $n = 1$ and (b) $n = 2$ for $\gamma_D = 0.3, \gamma_z = 0.1$, (c) $n = 1$, and (d) $n = 2$ for $\gamma_R = 0.3, \gamma_z = 0.1$, and $\gamma_{D,R} = 0.3, \gamma_z = 0$.

4. Conclusion

In conclusion, we have presented an exact analytical solution to the spin edge states, induced by the combined effect of BR SOI Zeeman effect or D SOI and Zeeman effect in a 2DES restricted by the hard-wall confining potential and exposed to a perpendicular quantizing magnetic field. The exact solution of the problem allows its deeper intuitive understanding and can be a strong input in studying the spin transport through edge channels. We have shown that the inclusion of Zeeman term leads to an increase or decrease in the splitting of energy levels. We calculate the spectral properties of spin edge states in the presence of Zeeman effect and find that due to SOI the spin edge states are resolved not only in the energy but are also separated spatially. From the obtained spectrum we calculate average spin components along x, y, z directions and show that in the case of Dresselhaus SOI and Zeeman interaction the electron spins are aligned along propagation direction of spin edge states, i.e. along the boundary of the sample. This is in contrast to the case of the Bychkov-Rashba SOI and Zeeman interaction where the spins are aligned perpendicular to the propagation direction of edge states.

Acknowledgments

I thank Prof. S. M. Badalyan for formulation of the research task.

References

1. **J. Fabian, A. Matos-Abiague, C. Ertler, P. Stano, and I. Žutić,** Acta Phys. Slov. **57**, 565 (2007).
2. **Žutić, J. Fabian, and S. Das Sarma,** Rev. Mod. Phys. **76**, 323 (2004).
3. **S. A. Wolf, D. D. Awschalom, R. A. Buhrman, J. M. Daughton, S. von Molnár, M. L. Roukes, A. Y. Chtchelkanova, and D. M. Treger,**Science **294**, 1488 (2001).
4. **M. I. D'yakonov and V. Yu. Kachorovskii**, Sov. Phys. Semicond., **20**, 110 (1986).
5. **Y. K. Kato, R. C. Myers, A. C. Gossard, and D. D. Awschalom,**Science **306**, 1910 (2004).
6. **S. M. Badalyan and G. Vignale,** *Phys. Rev. Lett.,* **103***,* 196601 (2009).
7. **C. P. Weber, N. Gedik, J. E. Moore, J. Orenstein, J. Stephens, and D. D. Awschalom,** Nature (London) **437**, 1330 (2005).
8. **S. M. Badalyan, C. S. Kim, and G. Vignale,**Phys. Rev. Lett. **100**, 016603 (2008).
9. **B. A. Bernevig, J. Orenstein, and S. C. Zhang**, Phys. Rev. Lett. **97**, 236601 (2006).
10. **S. M. Badalyan, A. Matos-Abiague, G. Vignale, and J. Fabian**, Phys. Rev. B **79**, 205305 (2009).
11. **B. Das, S. Datta, R. Reifenberger.**Phys. Rev. B, **41**, 8278 (1990).
12. **V.I. Fal'ko.** Phys. Rev. B, **46**, 4320 (1992).
13. **S.A. Tarasenko, N.S. Averkiev.** JETP Lett., **75**, 552 (2002).
14. **J. Schliemann, J.C. Egues, D. Loss.**Phys. Rev. B, **67**, 085302 (2003).
15. **V. Sih, W.H. Lau, R.C. Myers, A.C. Gossard, M.E. Flatte', D.D. Awshalom.** Phys. Rev. B, **70**, 161313(R) (2004).
16. **X.F.Wang, P. Vasilopoulos.**Phys. Rev. B,**72**, 085344 (2005).
17. **E. Lipparini, M. Barranco, F. Malet, M. Pi, L. Serra.** Phys. Rev. B, **74**, 115303 (2006).
18. **R.B. Laughlin.** Phys. Rev. B, **23**, 5632 (1981).
19. **B.I. Halperin.** Phys. Rev. B, **25**, 2185 (1982).
20. **A.H. MacDonald, P. Streda.**Phys. Rev. B, **29**, 1616 (1984).

21. **S.M. Badalyan, Y.B. Levinson, D.L. Maslov.** JETP Lett.,**53**, 619 (1991).
22. **Yun-Juan Bao, Huai-Bing Zhuang, Shun-Qing Shen, Fu-Chun Zhang.** Phys. Rev. B,**72**, 245323 (2005).
23. **Jun Wang, H.B. Sun, D.Y. Xing.**Phys. Rev. B,**69**, 085304 (2004).
24. **A. Reynoso, G. Usaj, M.J. Sanchez, C.A. Balseiro.** Phys. Rev. B,**70**, 235344 (2004).
25. **S. Debald, B. Kramer.** Phys. Rev. B,**71**, 115322 (2005).
26. **Anh T. Ngo, J.M. Villas-Bôas, Sergio E. Ulloa.** Phys. Rev. B,**78**, 245310 (2008).
27. **H. Su and B.-Y. Gu.** Phys. Lett. A,**341**, 198 (2005).
28. **V. L. Grigoryan, A. M. Abiague and S. M. Badalyan**, Phys. Rev. B,**80**, 165320 (2009)
29. **V.Ya. Aleshkin et al.**, FTP, 2008, **42(7)**, 846.